Journal of Electrochemical Energy Conversion and Storage, 17, 031006-1, 2020.

Improving Retention-Rate of NCA Cathode Material Synthesized Using Glycerol Solvent

Khaleel I. Hamad
Department of Chemical Engineering, University of Missouri, Columbia, MO 65211 (USA)
Kihkv9@mail.missouri.edu
Yangchuan Xing [1]
Department of Chemical Engineering, University of Missouri, Columbia, MO 65211 (USA)
xingy@missouri.edu

ABSTRACT

This paper reports an enhanced retention-rate of $LiNi_{0.8}Co_{0.15}Al_{0.05}O_2$ (NCA) cathode material for Li-ion batteries synthesized with glycerol as a solvent and a reactant. Glycerol is a fuel and the heat released during synthesis could be considered as an additional free source of material preparation. SEM images and XRD result show an early stage of crystallization of the produced powder. Early crystallization in the NCA material at low temperatures was believed to hinder cationic mixing that would occur at higher temperatures during calcination. As a result, cycling of the NCA material shows a very stable capacity. The NCA material displays 97% capacity retention at 1C (1C = 200 mA/g) after 50 cycles, 87.6% at 0.3C after 100 cycles, and 93.6% at 0.1C after 70 cycles, which are better than those reported previously.

Keywords: Li-ion Battery; NCA cathode material; Glycerol; Capacity retention.

[1] Corresponding author: xingy@missouri.edu (Y. Xing)

Introduction

Up to now, many synthesis approaches, such as co-precipitation[1,2], sol-gel method [3], solution combustion [4] and solid state reaction[5], have been tried to prepare the $LiNi_{0.8}Co_{0.15}Al_{0.05}O_2$ (NCA) cathode material to be used in lithium ion batteries (LIBs). Despite all the progress made in synthesis techniques, one of the most challenging problems is still to make an NCA material stable enough for commercial-scale applications.

Sol-gel synthesis route is one of the promising techniques that have been used widely to synthesize different Li-ion cathode materials. Although recent studies have not paid much attention to the sol-gel techniques to synthesize NCA cathode materials, this synthesis approach is still considered an efficient way to prepare nanoscale materials. Such techniques make an effective way to transform the highly soluble chemical compounds into chemically reactive forms of hydrated oxides during hydrolysis processing [6]. These hydrated oxides show considerable stability in the solution, which makes reproducibility of the materials possible, and the final products are easily purified, which in turns gives rise high chemical quality of the final products. However, there still some limitations of using the sol-gel technique nowadays because of the smaller secondary particle size that is produced by using water as a solvent.

Our previous work with using glycerol instead of water in this regard shows bigger particle size and better electrochemical activity compared with other proposed cathode materials [7,8]. In this communication, we report an NCA cathode material synthesized using glycerol. The glycerol is beneficial, unlike water, in forming crystalline structures at earlier stages in the synthesis, as observed in scanning electron microscopy (SEM) and X-ray diffraction (XRD). This is believed to reduce the cationic mixing during calcination of the powder at high temperatures. Consequently, the produced powders show very high retention-rate during cycling.

Experimental

NCA powders were synthesized by using a previously developed method,[7,8] in which stoichiometric amounts of Li $(CH_3COO)_2{\cdot}2H_2O$, Ni $(CH_3COO)_2{\cdot}4H_2O$, Co $(CH_3COO)_2{\cdot}4H_2O$, and Al $(NO_3)_3{\cdot}9H_2O$ were dissolved in glycerol as a deep eutectic solvent (DES) precursor at 80 °C with stirring. The DES precursor has a metal salt to glycerol molar ratio (M^+/Glycerol) of 1:3. To this DES precursor solution, cornstarch is added as a gelling agent at the same temperature with continuous stirring with a molar ratio (M^+/cornstarch) of 4:1. The gel forms afterward and the heating temperature was increased to 400 °C to obtain a dry NCA powder. The dry powder was then pelletized and introduced to a high temperature furnace for heat treatment of 750 °C for 12 hr in air at a heating rate of 5 °C/min. The calcined powder was grounded and used for further characterization studies.

The crystalline structure for the NCA powder was characterized by using XRD with the following measurement conditions: nickel-filtered Cu kα radiation (kα1 = 1.5405980 Å and kα2 = 1.5444 Å) and 2θ values ranging from 10° to 90° with a scan rate of 0.02°/s. The particle distribution and morphology were detected by using An Environmental Scanning Electron Microscope (SEM, FEI Quanta 600 FEG).

The electrochemical tests were all done by using 2032 coin-type cell, that was assembled in an argon-filled glove box (MBRAUN). The coin-type battery consists of a cathode material (positive electrode), anode material (negative electrode), a porous polypropylene separator (Celegard) between the two electrodes, and the electrolyte. The cathode material was made as follows: 80% active material, 10% polyvinylidene fluoride (PVDF), and 10% carbon black. The three materials were mixed first with a suitable amount of N-methyl-pyrrolidone (NMP) and then cast over an aluminum foil. The wet slurry then was dried in a furnace at 60 °C for 2 hr, followed by another drying in a vacuum furnace at 120 °C for 12 hr. A 7/16 inch of the dried cast is punched out and pressed between two aluminum meshes at 10 kN prior to the final battery assembly in glovebox. The lithium foil was used as the anode material in the size of ½ inch (circular shape). And the electrolyte was a mixture of 1M $LiPF_6$ dissolved in dimethyl carbonate (DMC) and ethylene carbonate (EC) at a volume ratio of 1:1.

The assembled cells were charged and discharged in an Arbin battery tester (Model BT-2043) at constant current densities of 0.1C for the initial cycle (1C = 200 mA/g), 0.3C and 1C for 100 cycles over the voltage range of 2.7-4.3 V. The rate capability was carried out at different current densities of 0.1C, 0.2C, 1C, 2C and 5C over the same voltage range. Camry Reference 3000 potentiostat was used to collect cyclic voltammetry between 2.7-4.3 V at 0.1 mV/s scanning rate, and the impedance measurement (EIS) was over a frequency range from 1 MHz to 0.01 Hz.

Results and discussion

SEM images of the dry powder and the calcined powder are displayed in Figure 1. The results of the dry powder before calcination show that there are pre-crystalline nanoparticles. The calcined powder (at 750 °C for 12 hr) show hexagonal and rectangular prismatic nanorod shape with size ranging from 0.26 to 0.80 µm.

Figure 2 (a) and (b) are the XRD patterns for both the dry powder and the calcined powder. As seen in Figure 2(a) there are clear crystalline peaks appeared at different diffraction angles, which are believed to be Li_2CO_3 and NiO. As the powder has been calcined at high temperatures, the peaks become more evident as shown in Figure 2 (b). For the calcined powder, the diffraction peaks can be indexed to a well-define layered structure of α-$NaFeO_2$ type with a space group of *R-3m*.

One of the most well-known issues in the layered structure material is the cationic mixing. The NCA material has 80% Ni, and as addressed in the literature Ni^{2+} is hard to be completely oxidized to Ni^{3+}, resulting in the presence of Ni^{2+} in the NCA material [9,10]. The similar size in ionic radii of both Li^+ and Ni^{2+} would trigger Ni^{2+} migration to the Li layer, impeding Li^+ diffusion during the charge/discharge processes [11]. The intensity ratio of $I_{(003)}/I_{(104)}$ in the layered structure was found to be related to the cationic mixing, and the value above 1.2 indicates a lower cationic mixing and vice versa [12]. The intensity ratio of 1.38 was found in our NCA material, indicating that the synthesized material has a low degree of cationic mixing. A clear hexagonal structure of the NCA material can be defined based on the distinct splitting peaks of (006)/(102) and (018)/(110) [13]. These results suggest that the synthesized powder using the DES precursor has a much better cationic ordering, and the initial crystallization of the powder can mitigate the cationic mixing at high temperatures.

To demonstrate the electrochemical stability and performance, electrochemical tests are conducted in the voltage range of 2.7-4.3 V as displayed in Figure 3. The initial charge-discharge curves at 0.1C are presented in Figure 3(a). The NCA material delivers an initial discharge capacity of 174.82 mAh/g. Further tests were conducted at different rates of 0.3C and 1C for 100 cycles, as shown in Figure 3(b).

The results show very high capacity retention rates of 87.6% at 0.3C (163.00 mAh/g at 1^{st} and 142.88 mAh/g at 100^{th}) and 87.3% at 1C (131.92 mAh/g at 1^{st} and 115.22 mAh/g at 100^{th}). The rate capability of the cell is carried out at different current densities and returns to the 0.1C for 70 cycles (60-120^{th} cycle) with superior capacity retention of 93.6% as shown in Figure 3(c).

The high stability of the NCA cathode material could be attributed to the better cationic ordering of the NCA cathode material using glycerol, which diminishes cationic mixing when crystalline structures are formed at early stages in heat treatment as explained earlier. Comparing with other NCA cathode materials made using different methods, this synthesis approach using a DES precursor has shown an appreciated improvement in electrochemical performance as can be further seen in Table 1.

Figure 4 (a) shows the voltammograms of the NCA material in the potential range of 2.7-4.3V (vs. Li^+/Li) at 0.1 mV/s for the 1^{st}, 2^{nd}, and the 10^{th} cycles. There are three anodic and three cathodic peaks observed in this Figure. The peaks are attributed to the phase transitions from the hexagonal phase to the monoclinic phase, the monoclinic phase to the hexagonal phase, and the hexagonal phase to the hexagonal phase during the charge/discharge processes [14–16]. The electrode polarization is minimized as it moves from the 1^{st} cycle to the 2^{nd} and then the 10^{th} cycles, indicative of larger reversibility of Li+ during the intercalation/ deintercalation processes [17]. Notably, the second and third oxidation peaks are more evident in the 10^{th} cycle than the 1^{st} and 2^{nd} cycles. This could be attributed to the lowest cationic mixing that associated with the highest reversibility in phase transitions [18]. Figure 4(b) illustrates the electrochemical impedance spectra (EIS) for the NCA cathode material at fully discharged state of 2.7 V after the 10^{th} cycle. The charge resistance (R_{ct}) of the cathode material shows a very low resistance of 13.4 Ω after the 10^{th} cycle.

Summary

Layered NCA cathode material synthesized by using glycerol solvent was shown to have very good retention rate. The electrochemical results show 97/87.3%, 87.6/93.2% discharge capacity retention after 50/100 cycles at 1C and 1/3C, respectively in the voltage range between 2.7-4.3 V. After cycling the cell at different rates for 50 cycles and going back to 0.1C discharge rate, 93.6% of the 51^{st} discharge capacity has been retained at the end of the 120^{th} cycle. The superior performances are ascribed to the well-ordered metal oxides with less cationic mixing and higher reversibility, which is a result of early crystallization in the NCA material synthesized using glycerol as solvent.

Acknowledgement

This material is based upon work partially supported by the Department of Energy Office of Energy Efficiency and Renewable Energy (EERE), under Award Number DE-EE0007282. They also acknowledge partial financial support from the University of Missouri. K.I.H would like to thank the Higher Committee for Education Development in Iraq (HCED) for providing a scholarship. The authors would to thank Dr. Eric Bohannan for help with obtaining XRD results.

References

[1] Liu, W. M., Hu, G. R., Peng, Z. D., Du, K., Cao, Y. B., and Liu, Q., 2011, "Synthesis of Spherical $LiNi_{0.8}Co_{0.15}Al_{0.05}O_2$ Cathode Materials for Lithium-Ion Batteries by a Co-Oxidation-Controlled Crystallization Method," Chinese Chemical Letters, **22**(9), pp. 1099–1102.

[2] Wu, N., Wu, H., Yuan, W., Liu, S., Liao, J., and Zhang, Y., 2015, "Facile Synthesis of One-Dimensional $LiNi_{0.8}Co_{0.15}Al_{0.05}O_2$ Microrods as Advanced Cathode Materials for Lithium Ion Batteries," J. Mater. Chem. A, **3**(26), pp. 13648–13652.

[3] Han, C. J., Yoon, J. H., Cho, W. I., and Jang, H., 2004, "Electrochemical Properties of $LiNi_{0.8}Co_{0.2-x}Al_xO_2$ Prepared by a Sol–Gel Method," Journal of Power Sources, **136**(1), pp. 132–138.

[4] Majumder, S. B., Nieto, S., and Katiyar, R. S., 2006, "Synthesis and Electrochemical Properties of $LiNi_{0.80}(Co_{0.20-x}Al_x)O_2$ (X=0.0 and 0.05) Cathodes for Li Ion Rechargeable Batteries," Journal of Power Sources, **154**(1), pp. 262–267.

[5] Xia, S., Zhang, Y., Dong, P., and Zhang, Y., 2014, "Synthesis Cathode Material $LiNi_{0.80}Co_{0.15}Al_{0.05}O_2$ with Two Step Solid-State Method under Air Stream," The European Physical Journal - Applied Physics, **65**(1).

[6] Sakka, S., and Kozuka, H., 2005, *Handbook of Sol-Gel Science and Technology. 1. Sol-Gel Processing*, Springer Science & Business Media.

[7] Hamad, K. I., and Xing, Y., 2018, "Effect of Cobalt and Nickel Contents on the Performance of Lithium Rich Materials Synthesized in Glycerol Solvent," J. Electrochem. Soc., **165**(11), pp. A2470–A2475.

[8] Hamad Khaleel I., Liao Jin-Yun, Smith Taylor W., and Xing Yangchuan, 2017, "Synthesis of Layered $LiMn_{1/3}Ni_{1/3}Co_{1/3}O_2$ Oxides for Lithium-Ion Batteries Using Biomass-Derived Glycerol as Solvent," Energy Technology, **6**(4), pp. 710–717.

[9] Li, X., Xie, Z., Liu, W., Ge, W., Wang, H., and Qu, M., 2015, "Effects of Fluorine Doping on Structure, Surface Chemistry, and Electrochemical Performance of $LiNi_{0.8}Co_{0.15}Al_{0.05}O_2$," Electrochimica Acta, **174**, pp. 1122–1130.

[10] Hua, C., Du, K., Tan, C., Peng, Z., Cao, Y., and Hu, G., 2014, "Study of Full Concentration-Gradient $Li(Ni_{0.8}Co_{0.1}Mn_{0.1})O_2$ Cathode Material for Lithium Ion Batteries," Journal of Alloys and Compounds, **614**, pp. 264–270.

[11] Bianchi, V., Caurant, D., Baffier, N., Belhomme, C., Chappel, E., Chouteau, G., Bach, S., Pereira-Ramos, J. P., Sulpice, A., and Wilmann, P., 2001, "Synthesis, Structural Characterization and Magnetic Properties of Quasistoichiometric $LiNiO_2$," Solid State Ionics, **140**(1), pp. 1–17.

[12] Tan, L., and Liu, H., 2010, "High Rate Charge–Discharge Properties of $LiNi_{1/3}Co_{1/3}Mn_{1/3}O_2$ Synthesized via a Low Temperature Solid-State Method," Solid State Ionics, **181**(33–34), pp. 1530–1533.

[13] Lu, Z., Beaulieu, L. Y., Donaberger, R. A., Thomas, C. L., and Dahn, J. R., 2002, "Synthesis, Structure, and Electrochemical Behavior of $Li[Ni_xLi_{1/3-2x/3}Mn_{2/3-x/3}]O_2$," J. Electrochem. Soc., **149**(6), pp. A778–A791.

[14] Lim, S. N., Ahn, W., Yeon, S.-H., and Park, S. B., 2014, “Enhanced Elevated-Temperature Performance of $Li(Ni_{0.8}Co_{0.15}Al_{0.05})O_2$ Electrodes Coated with Li_2O-B_2O_3 Glass,” Electrochimica Acta, **136**, pp. 1–9.
[15] Kojima, Y., Muto, S., Tatsumi, K., Kondo, H., Oka, H., Horibuchi, K., and Ukyo, Y., 2011, “Degradation Analysis of a Ni-Based Layered Positive-Electrode Active Material Cycled at Elevated Temperatures Studied by Scanning Transmission Electron Microscopy and Electron Energy-Loss Spectroscopy,” Journal of Power Sources, **196**(18), pp. 7721–7727.
[16] Oh, S. H., Lee, S. M., Cho, W. I., and Cho, B. W., 2006, “Electrochemical Characterization of Zirconium-Doped $LiNi_{0.8}Co_{0.2}O_2$ Cathode Materials and Investigations on Deterioration Mechanism,” Electrochimica Acta, **51**(18), pp. 3637–3644.
[17] Xiong, X., Ding, D., Wang, Z., Huang, B., Guo, H., and Li, X., 2014, “Surface Modification of $LiNi_{0.8}Co_{0.1}Mn_{0.1}O_2$ with Conducting Polypyrrole,” J Solid State Electrochem, **18**(9), pp. 2619–2624.
[18] Park, T.-J., Lim, J.-B., and Son, J.-T., 2014, “Effect of Calcination Temperature of Size Controlled Microstructure of $LiNi_{0.8}Co_{0.15}Al_{0.05}O_2$ Cathode for Rechargeable Lithium Battery,” Bulletin of the Korean Chemical Society, **35**(2), pp. 357–364.
[19] Li, Y., Yu, H., Hu, Y., Jiang, H., and Li, C., 2018, “Surface-Engineering of Layered $LiNi_{0.815}Co_{0.15}Al_{0.035}O_2$ Cathode Material for High-Energy and Stable Li-Ion Batteries,” Journal of Energy Chemistry, **27**(2), pp. 559–564.
[20] Wu, G., and Zhou, Y., 2019, “TiP_2O_7-Coated $LiNi_{0.8}Co_{0.15}Al_{0.05}O_2$ Cathode Materials with Improved Thermal Stability and Superior Cycle Life,” Journal of Energy Chemistry, **28**, pp. 151–159.
[21] Tian, L., Liang, K., Wen, X., Shi, K., and Zheng, J., 2018, “Enhanced Cycling Stability and Rate Capability of $LiNi_{0.80}Co_{0.15}Al_{0.05}O_2$ Cathode Material by a Facile Coating Method,” Journal of Electroanalytical Chemistry, **812**, pp. 22–27.
[22] Xia, S., Li, F., Chen, F., and Guo, H., 2018, “Preparation of $FePO_4$ by Liquid-Phase Method and Modification on the Surface of $LiNi_{0.80}Co_{0.15}Al_{0.05}O_2$ Cathode Material,” Journal of Alloys and Compounds, **731**, pp. 428–436.
[23] Qiu, Z., Zhang, Y., Dong, P., Xia, S., and Yao, Y., 2017, “A Facile Method for Synthesis of $LiNi_{0.8}Co_{0.15}Al_{0.05}O_2$ Cathode Material,” Solid State Ionics, **307**, pp. 73–78.

Figure Captions List

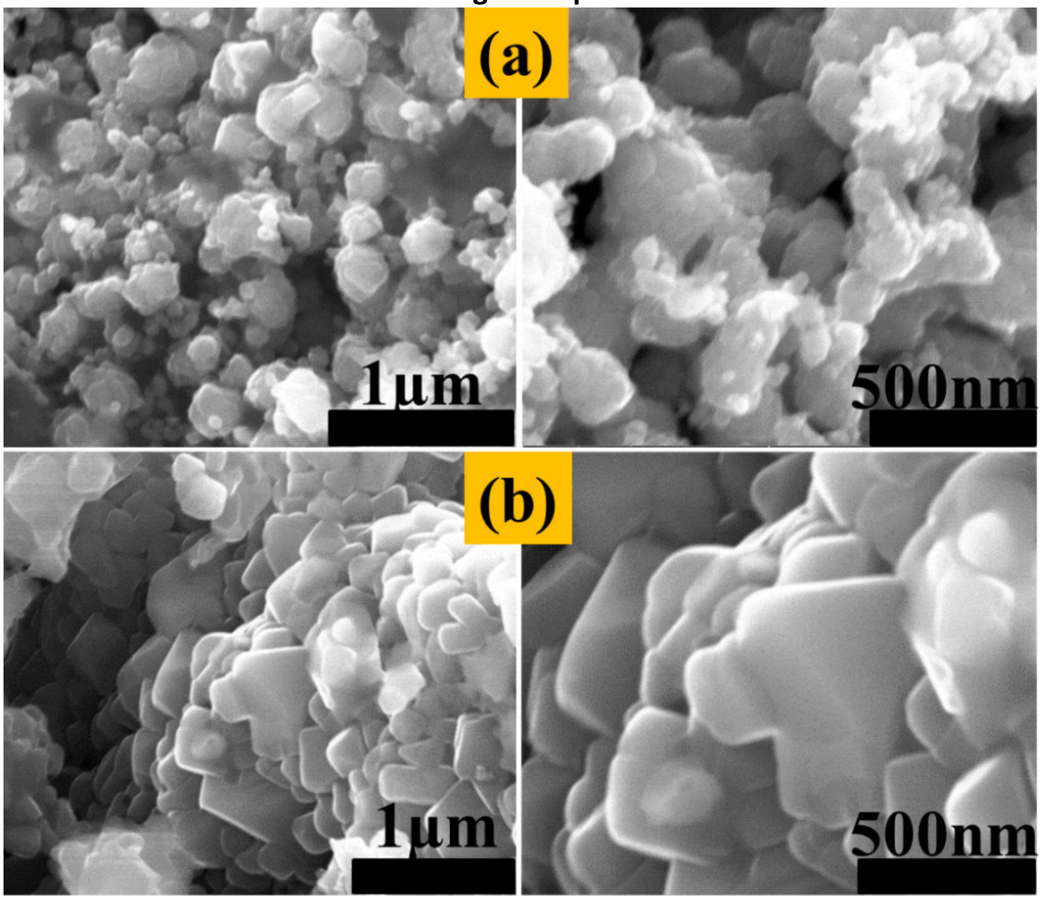

Fig. 1 The SEM images of the dry powder (a), and the sintered one at 750 °C for 12 hr (b).

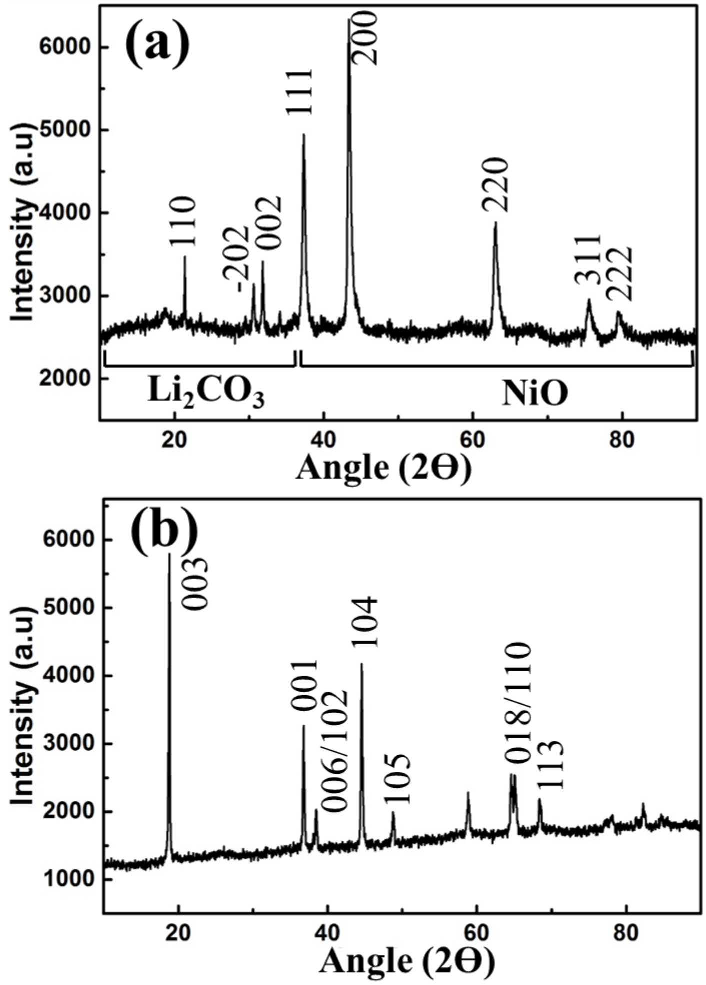

Fig. 2 Figure 2. XRD patterns for (a) dry powder (400 °C) and (b) calcined powder at 750 °C for 12 hr.

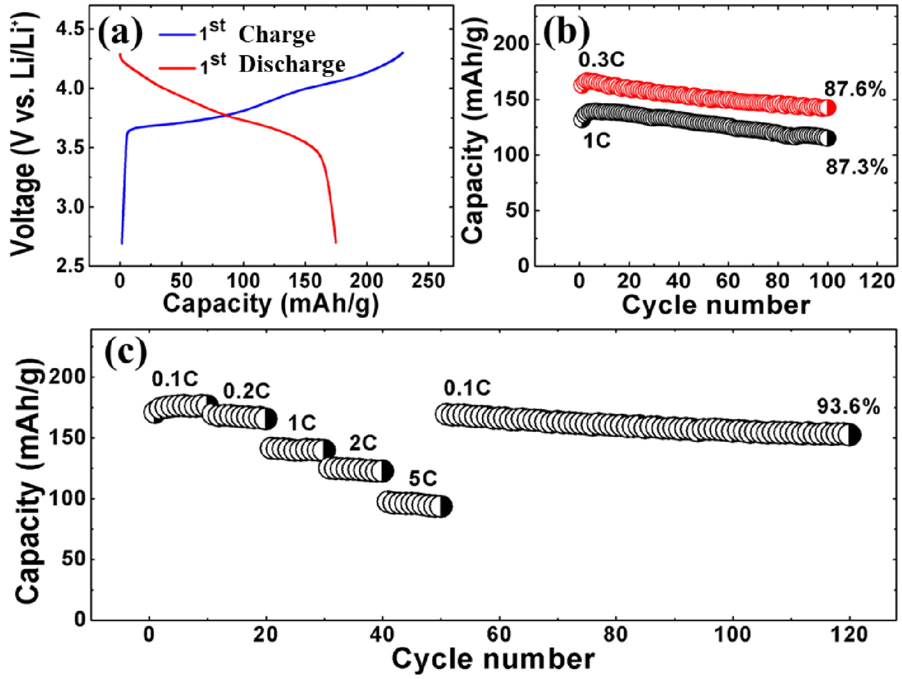

Fig.3. (a) Initial charge/discharge capacity at 0.1C, (b) discharge capacity at 0.3 and 1C, and (c) rate capability at different C-rates.

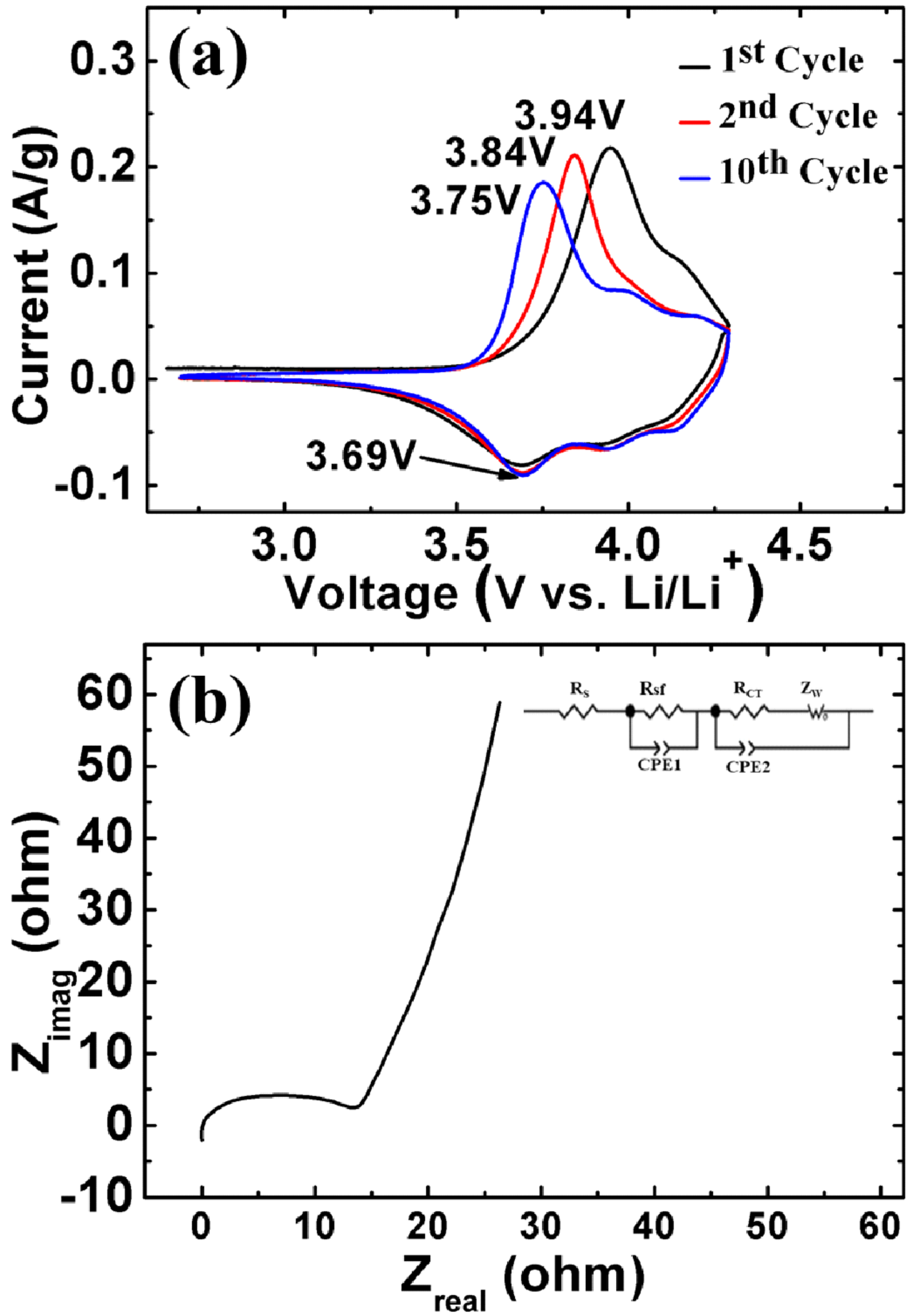

Fig.4 (a) Cyclic voltammetry for the 1st, 2nd and the 10th cycles, (b) Nyquist plot after the 10th cycle of the NCA cathode material.

Table 1. Comparison of NCA cathode material electrochemical performance with previous work.

Synthesis method	Retention Rate	Reference
Ball-milling	80.9%, 1C at 100 cycles	[19]
Co-precipitation	79.9%, 0.5C after 100cycles	[20]
Co-precipitation	86.1%, 1C at 60 cycles	[21]
Solid-state at 750℃/24 h	77.36%,1C at 60 cycles	[22]
Solid-state at 750℃/24 h	92%, 1C at 60 cycles	[23]
Sol-gel at 800℃/24 h	91%, 0.5C at 50 cycles	[3]
DES precursor at 750℃/12 h	93.6%, 0.1C at 50-120 cycles 93.2% and 87.6%, 0.3 C at 50 and 100 cycles 97% and 87.3%, 1C at 50 and 100 cycles	This study